Pflügers Archiv - European Journal of Physiology (2018) 470:1377–1389
https://doi.org/10.1007/s00424-018-2156-6

NEUROSCIENCE

Metabolic modulation of neuronal gamma-band oscillations

Wadim Vodovozov[1] · Justus Schneider[1] · Shehabeldin Elzoheiry[1] · Jan-Oliver Hollnagel[1] · Andrea Lewen[1] · Oliver Kann[1,2]

Received: 5 December 2017 / Revised: 6 April 2018 / Accepted: 17 May 2018 / Published online: 28 May 2018

Abstract

Gamma oscillations (30–100 Hz) represent a physiological fast brain rhythm that occurs in many cortex areas in awake mammals, including humans. They associate with sensory perception, voluntary movement, and memory formation and require precise synaptic transmission between excitatory glutamatergic neurons and inhibitory GABAergic interneurons such as parvalbumin-positive basket cells. Notably, gamma oscillations are exquisitely sensitive to shortage in glucose and oxygen supply (metabolic stress), with devastating consequences for higher cognitive functions. Herein, we explored the robustness of gamma oscillations against changes in the availability of alternative energy substrates and amino acids, which is partially regulated by glial cells such as astrocytes. We used organotypic slice cultures of the rat hippocampus expressing acetylcholine-induced persistent gamma oscillations under normoxic recording conditions (20% oxygen fraction). Our main findings are (1) partial substitution of glucose with pyruvate and the ketone body β-hydroxybutyrate increases the frequency of gamma oscillations, even at different stages of neuronal tissue development. (2) Supplementation with the astrocytic neurotransmitter precursor glutamine has no effect on the properties of gamma oscillations. (3) Supplementation with glycine increases power, frequency, and inner coherence of gamma oscillations in a dose-dependent manner. (4) During these treatments switches to other frequency bands or pathological network states such as neural burst firing or synchronized epileptic activity are absent. Our study indicates that cholinergic gamma oscillations show general robustness against these changes in nutrient and amino acid composition of the cerebrospinal fluid; however, modulation of their properties may impact on cortical information processing under physiological and pathophysiological conditions.

Keywords Astrocyte · Electrophysiology · Energy metabolism · Neuromodulation · Neuronal activity · Slice cultures

Introduction

Neuronal network oscillations in the gamma-frequency band (30–100 Hz) emerge in many cortical areas, usually during wakefulness in mammals, including humans. Such gamma oscillations have been associated with higher cognitive functions, such as sensory perception, attentional selection, voluntary movement, and memory formation [45, 76]. Gamma oscillations significantly rely on rhythmic perisomatic inhibition of pyramidal cells by GABAergic interneurons, such as parvalbumin-positive basket cells [29, 45]. Notably, gamma oscillations are associated with high energy expenditure and show exquisite sensitivity to metabolic and oxidative stress [41, 44, 62, 69].

The mammalian brain is an organ with a high metabolic rate. In humans, the brain uses about 20% of the oxygen and about 25% of the glucose at rest [8]. Glucose has been considered the dominant exogenous energy substrate in the adult brain [19, 66]. Having a role in different biochemical pathways, glucose metabolism has important functions related to bioenergetics, neurotransmission, and oxidation–reduction (redox) reactions in the brain parenchyma [6, 19, 42].

However, the brain is capable to use energy substrates other than glucose during postnatal development as well as in ordinary or clinical situations such as exhaustive physical exercise, long-term starvation, and diabetes mellitus [3, 17, 34, 57, 66]. Experimental studies using brain slices also showed that alternative energy substrates can sustain—or even enhance—

✉ Oliver Kann
oliver.kann@physiologie.uni-heidelberg.de

[1] Institute of Physiology and Pathophysiology, University of Heidelberg, Im Neuenheimer Feld 326, 69120 Heidelberg, Germany

[2] Interdisciplinary Center for Neurosciences (IZN), University of Heidelberg, 69120 Heidelberg, Germany

energy metabolism and thus synaptic neuronal functions under certain experimental conditions [24, 37, 38, 70, 78]. Prominent examples are monocarboxylates, such as lactate and pyruvate, as well as the ketone body β-hydroxybutyrate, the levels of which are partially regulated by glial cells, such as astrocytes [1, 2, 34, 54, 77].

In the present study, we explored the robustness of gamma oscillations against changes in the composition of available energy substrates and amino acids, which can occur in physiological and pathophysiological conditions [1, 3, 17, 57, 66].

We used organotypic hippocampal slice cultures of the rat that were maintained on Biopore™ membranes in an interface recording chamber. This experimental approach permits the investigation of persistent gamma oscillations in normoxic recording condition (20% oxygen fraction) as well as efficient exchange of energy substrates and drugs in the tissue [25, 36, 68]. We focused on the alternative energy substrates pyruvate and β-hydroxybutyrate as well as the amino acids glutamine and glycine that have a central role in synaptic neurotransmission [30, 46, 66].

Materials and methods

Ethical statement

Rats were purchased from Charles-River (Sulzfeld, Germany) and handled in accordance with the European directive 2010/63/EU and with consent of the animal welfare officers at the University of Heidelberg (licenses, T46/14 and T96/15). Experiments were performed and reported in accordance with the ARRIVE guidelines.

Slice cultures and recording chamber with 20% oxygen fraction

Organotypic hippocampal slice cultures were prepared as described [43, 68]. In brief, hippocampal slices (400 μm) were cut with a McIlwain tissue chopper (Mickle Laboratory Engineering Company Ltd., Guildford, UK) from 10-day-old Wistar rats under sterile conditions. Slices with intact hippocampal structures were maintained on Biopore™ membranes (Millicell standing inserts, Merck Millipore, Darmstadt, Germany) between culture medium, which consisted of 50% minimal essential medium, 25% Hank's balanced salt solution (Sigma-Aldrich, Taufkirchen, Germany), 25% heat-inactivated horse serum (Life Technologies, Darmstadt, Germany), and 2 mM L-glutamine (Life Technologies) at pH 7.3 titrated with Trisbase, and humidified normal atmosphere (5% CO_2, 36.5 °C) in an incubator (Heracell, Thermoscientific, Dreieich, Germany). The calculated glucose concentration in the culture medium was about 4 mM. Biopore™ membranes provide high viability and excellent transmissibility of gases and substrates. The culture medium (1 ml) was replaced three times per week. Slice cultures were used after 11–28 days in vitro (DIV), when the tissue had recovered from slice preparation and damaged cut surfaces had been re-organized [42, 68].

For recordings, the intact Biopore™ membrane carrying slice cultures was inserted into the recording chamber [36]. Slice cultures were maintained at the interface between recording solution and ambient gas mixture. Intact Biopore™ membrane inserts ensure efficient supply of oxygen, energy substrates, and drugs through the recording solution that flows underneath (rate 1.8 ml/min). The interface condition permits constant oxygen supply from the ambient gas mixture (20% O_2 and 5% CO_2, rate 1.5 l/min); in one control experiment, we used a different gas mixture (95% O_2 and 5% CO_2). In our standard experimental setting (20% O_2 and 5% CO_2), the oxygen partial pressure (pO_2) ranges from 140 mmHg (slice surface) to about 20 mmHg (slice core) during cholinergic gamma oscillations [36], thus being close to conditions in vivo [69]. The use of Biopore™ membranes in the interface recording chamber also permits efficient tissue saturation of energy substrates and drugs, such as the voltage-gated Na^+-channel blocker tetrodotoxin, in about 5 min [25].

Recording solutions and drugs

Slice cultures were constantly supplied with pre-warmed recording solution (artificial cerebrospinal fluid, ACSF). ACSF contained 129 mM NaCl, 3 mM KCl, 1.25 mM NaH_2PO_4, 1.8 mM $MgSO_4$, 1.6 mM $CaCl_2$, 21 mM $NaHCO_3$, and 10 mM glucose [43, 68]. For experiments on alternative energy substrates, 10 mM glucose was replaced with 5 mM glucose, 5 mM Na-pyruvate, and 4 mM Na-β-hydroxybutyrate [37]; for experiments on amino acids, glutamine (1 mM) or glycine (0.5, 1.5, and 2.5 mM) was added to the ACSF. The pH was 7.3 when the recording solution was saturated with gas mixtures containing 5% CO_2. Recordings were performed at 34 ± 1 °C.

Gamma oscillations were induced by continuous bath application of the cholinergic receptor agonist acetylcholine (2 μM) and the acetylcholine-esterase inhibitor physostigmine (400 nM) (cholinergic model) [36, 44]. In a subset of experiments, the glutamatergic receptor agonist kainic acid (100 nM) was used (glutamatergic model) [68]. Standard salts, acetylcholine, Na-pyruvate, Na-β-hydroxybutyrate, strychnine hydrochloride, and glycine were purchased from Sigma-Aldrich, physostigmine was from Tocris (R&D Systems GmbH, Wiesbaden-Nordenstadt, Germany), kainic acid was from Biotrend (Köln, Germany), and glutamine from Life Technologies (Darmstadt, Germany).

Recordings of local field potentials

The local field potential (LFP) was recorded with glass electrodes (resistance of 1–2 MΩ) filled with ACSF, which were made from GB150F-8P borosilicate filaments (Science Products GmbH, Hofheim, Germany) using a Zeitz DMZ Puller (Zeitz-Instruments Vertriebs GmbH; Martinsried, Germany). The electrode was positioned mainly in *stratum pyramidale* of the CA3 region with a mechanical micromanipulator (MM 33, Märzhäuser, Wetzlar, Germany). Local field potentials were recorded with an EXT 10-2F amplifier in EPMS-07 housing (npi electronic GmbH, Tamm, Germany), low-pass filtered at 3 kHz, and digitized at 10 kHz using a CED 1401 interface and Spike2 software (Cambridge Electronic Design, Cambridge, UK) for offline analysis.

Toluidine blue and parvalbumin staining

For immunohistochemistry of parvalbumin-positive interneurons, slice cultures were fixed overnight with 4% paraformaldehyde in phosphate-buffered salt solution (PBS), incubated for 5 h in 30% sucrose (AppliChem GmbH, Darmstadt, Germany), and cut in thin sections (25 μm) with a CM1850 cryostat (Leica Microsystems GmbH, Nussloch, Germany). Unspecific immunoglobulin reactions were blocked with 10% normal horse serum (Gibco) for 1 h. The primary antibody was mouse anti-parvalbumin (Sigma-Aldrich) and the secondary antibody was biotinylated horse anti-mouse (Vector Laboratories Inc., CA, USA). Sections were incubated with the primary antibody overnight at 4 °C under light-protected conditions. Lyophilized bovine serum albumin (Carl Roth GmbH & Co. KG, Karlsruhe, Germany) diluted to 0.2% in PBS served as blocking solution and as secondary antibody carrier protein. The secondary antibody was applied overnight at 4 °C under light-protected conditions. Afterwards, the sections were incubated for 2 h with 0.5% avidin and biotinylated horseradish peroxidase (Vectastain Elite ABC Kit, Vector Laboratories). Antibody binding was visualized by adding 0.05% diaminobenzidine substrate, 0.3% ammonium nickel sulphate in 0.05 M Trisbase 7–9®, and 0.003% H_2O_2 for < 5 min. The reaction was stopped by adding PBS (when the brown color was intense enough). Stained sections were placed on object plates and dried overnight. Sections were exposed to an ascending ethanol series and then maintained in xylol (Sigma-Aldrich) for 10 min prior to embedding with Entellan®Neu (Merck Millipore, Schwalbach, Germany).

For toluidine blue staining (Sigma-Aldrich), the slices were mounted on slides, exposed to descending ethanol series, briefly rinsed in double-distilled water, and then incubated in 0.1% toluidine blue working solution (pH 2.3) for 5–10 min. Thereafter, the slices were briefly rinsed in double-distilled water. Ninety-six percent ethanol with traces of glacial acetic acid was used for color differentiation of the staining. The sections were then exposed to ascending ethanol series, a 1:1 mixture of 100% ethanol and xylol and finally xylol for 10 min. Afterwards, the slices were embedded with Entellan®Neu (Merck Millipore, Schwalbach, Germany).

Data analysis and statistics

Offline signal analysis of gamma oscillations was performed in MATLAB 15a (The MathWorks, Inc., Natick, MA, USA). Data segments of 3 min were low-pass filtered with a digital Butterworth algorithm at 200 Hz corner frequency and processed with Welch's algorithm with a Hamming window size of 4096 points for calculation of the power spectral density (PSD) (bin size = 2.441 Hz).

Gamma oscillations were analyzed for various parameters, i.e., peak power spectral density (power), peak frequency (frequency), full width at half maximum (FWHM), and decay constant of the autocorrelation (decay of autocorrelation). Frequency distributions for 1 s sample traces are shown using Morlet wavelet transforms. Each recording lasted for about 60 min; the first half (0 to 30 min) served as control (ACSF). The analysis was performed in 3-min data segments of fully established, persistent gamma oscillations (27 to 30 min, ACSF) and after another 18 min in the presence of either alternative energy substrates or amino acids supplemented to the ACSF (45 to 48 min). Recordings were mainly done in the presence of acetylcholine and physostigmine [36, 44].

The data derived from (*n*) slice cultures and (*N*) preparations of rats are presented using boxplots: the median is shown by the horizontal gray line, and the bottom and top edges of the box indicate the 25th-percentile (q_1) and the 75th-percentile (q_2). The whiskers of the boxplot extent to the most extreme data points not considered as outliers. Outliers are defined as data points larger than $q_2 + (q_2\text{-}q_1)*1.5$ or less than $q_1\text{-}(q_2\text{-}q_1)*1.5$ and are plotted individually using +-symbols. Statistical significance ($p < 0.05$) was determined using SigmaPlot 12.5 (Systat Software, Inc., San Jose, CA, USA). Data distribution was tested for normality with Shapiro-Wilk test. Comparisons between paired data were made with paired *t* test and Wilcoxon signed rank test or with one-way repeated-measures ANOVA with Holm-Sidak post-hoc test as indicated. Figures were generated using MATLAB 15a (The MathWorks) and CorelDRAW (Corel Corporation, Ottawa, Ontario, Canada).

Results

Cholinergic gamma oscillations under normoxic recording conditions

Organotypic hippocampal slice cultures of the rat showed well-preserved *stratum pyramidale* in the CA3 and the CA1

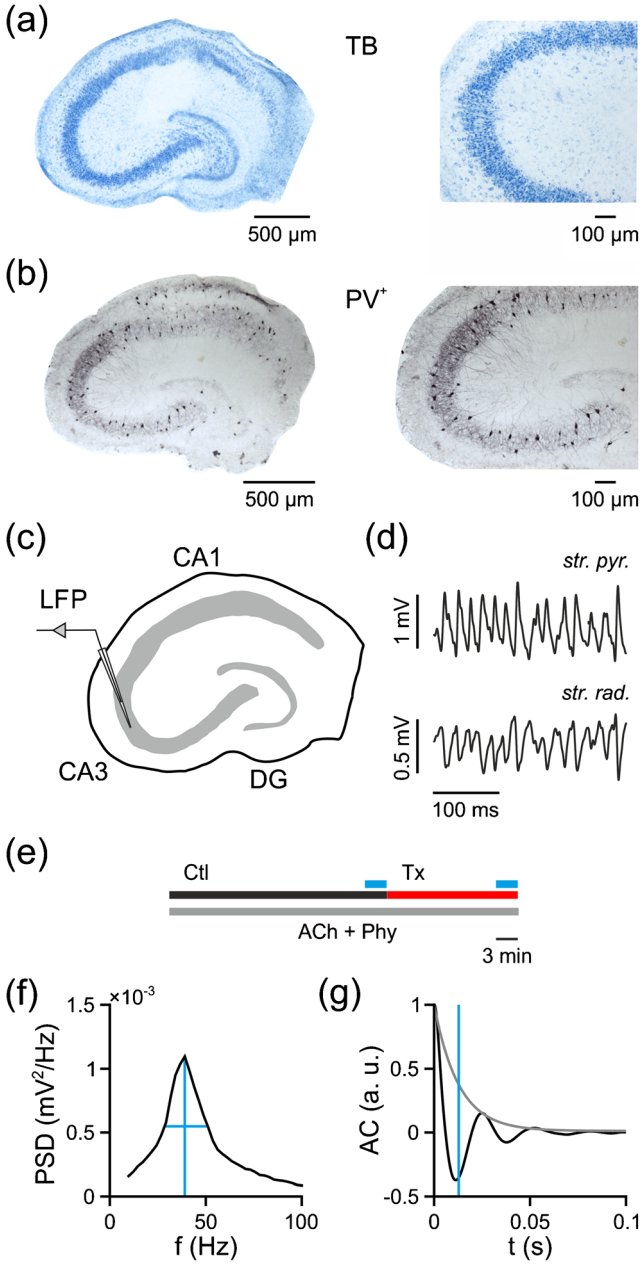

◀ **Fig. 1** Cholinergic gamma oscillations in hippocampal slice cultures of the rat. **a** Slice culture (10 DIV) stained with toluidine blue (TB) at low (left) and higher magnification (right). **b** Slice culture (10 DIV) with immunohistochemistry of parvalbumin-positive (PV^+) GABAergic interneurons at low (left) and higher magnification (right). Note that parvalbumin-positive GABAergic interneurons such as basket cells are crucial for the generation of gamma oscillations. **c** The scheme indicates the position of the extracellular local field potential (LFP) electrode in *stratum pyramidale* of the CA3 region. **d** Sample traces of gamma oscillations (200 Hz low-pass filtered) recorded simultaneously in *stratum pyramidale* (*str. pyr.*) and *stratum radiatum* (*str. rad.*) in CA3. **e** The scheme shows the general experimental protocol. Gamma oscillations were induced by continuous application of acetylcholine (2 µM) and physostigmine (400 nM) (ACh + Phy, lower gray bar) with the ACSF under normoxic recording conditions (20% oxygen fraction). The properties of gamma oscillations in control condition (Ctl, black line) were compared to the respective treatment (Tx, red line) with either alternative energy substrates or amino acids. Note that oscillation properties (**f**, **g**) were determined from data segments of the last 3 min of each condition (cyan bars at 27–30 and 45–48 min, respectively). **f** Power spectral density (PSD) calculated for gamma oscillations. Peak power (power, vertical cyan line), peak frequency (f, vertical cyan line) and full width at half maximum (FWHM, horizontal cyan line) were estimated from each power spectral density calculation. **g** Autocorrelation (AC, black curve) calculated for gamma oscillations. The peaks of the autocorrelation were fitted with an exponential decay function (gray curve) to estimate the decay constant of the autocorrelation (decay). The vertical cyan line marks the decay constant on the time axis

region and *stratum granulare* in the dentate gyrus (Fig. 1a, b). Moreover, immunohistochemistry revealed the complex network of parvalbumin-positive GABAergic interneurons that contact the perisomatic region of excitatory pyramidal cells in *stratum pyramidale* (Fig. 1b). Notably, parvalbumin-positive, fast-spiking interneurons such as basket cells are crucial for the generation of gamma oscillations [29, 45].

The use of slice cultures on an intact Biopore™ membrane in the interface recording chamber permitted to study neuronal network activity, even at normoxic atmosphere (20% oxygen fraction). Indeed, local field potential recordings in *stratum pyramidale* of the intrinsic hippocampal generator CA3 region revealed that bath application of acetylcholine and physostigmine resulted in persistent gamma oscillations, with an average frequency of around 40 Hz (Fig. 1c–e). The field potential reversal occurred between *stratum pyramidale* (pyramidal cell layer) and *stratum radiatum* (apical dendritic layer of pyramidal cells) (Fig. 1d). Calculations of the power spectral density (Fig. 1f) and the autocorrelation (Fig. 1g) were used for further analysis of the properties of gamma oscillations, i.e., power, frequency, FWHM, and decay of autocorrelation. Power, FWHM, and decay of autocorrelation reflect the number and synchronization of activated GABAergic synapses as well as the inner coherence of the oscillation [69, 73].

These data show that slice cultures feature well-preserved laminated tissue architecture and neuronal morphology and can reliably express cholinergic gamma oscillations at around 40 Hz, similar to acute hippocampal slices and the hippocampus in vivo [11, 21, 44, 45]. Moreover, the use of slice cultures permits the investigation of gamma oscillations under normoxic conditions, close to the physiological range [36, 69].

Application of pyruvate and β-hydroxybutyrate

We explored the effects of alternative energy substrates on gamma oscillations. For this purpose, glucose was partially substituted with exogenous pyruvate and the ketone body β-hydroxybutyrate [1, 28, 37, 47]. We performed these experiments in slice cultures at two different stages of tissue maturation to also address developmental aspects of neuronal

energy metabolism in rats [57, 77]. Notably, the state of maturation of organotypic hippocampal slice cultures at 11–14 DIV and at 28 DIV corresponds to the rat hippocampus in vivo during and after the suckling period, respectively [12, 18, 57, 75].

Gamma oscillations persisted in the presence of pyruvate and β-hydroxybutyrate at 11–14 DIV (Fig. 2a, b) as well as at 28 DIV (Fig. 2c, d). Switches to other frequency bands or neural bursts were absent. The most prominent effect of these alternative energy substrates was the increase in the frequency of gamma oscillations by about 4 Hz (Fig. 3b). Power, FWHM, and decay of autocorrelation were almost unaffected (Fig. 3a, c, d). In control experiments, i.e., slice cultures maintained in ACSF with acetylcholine and physostigmine, we excluded that the properties of gamma oscillations generally change during the respective time domain in the interface recording chamber (Fig. 3i–l, "Materials and methods" section).

We observed a similar effect of pyruvate and β-hydroxybutyrate on gamma oscillation frequency in further

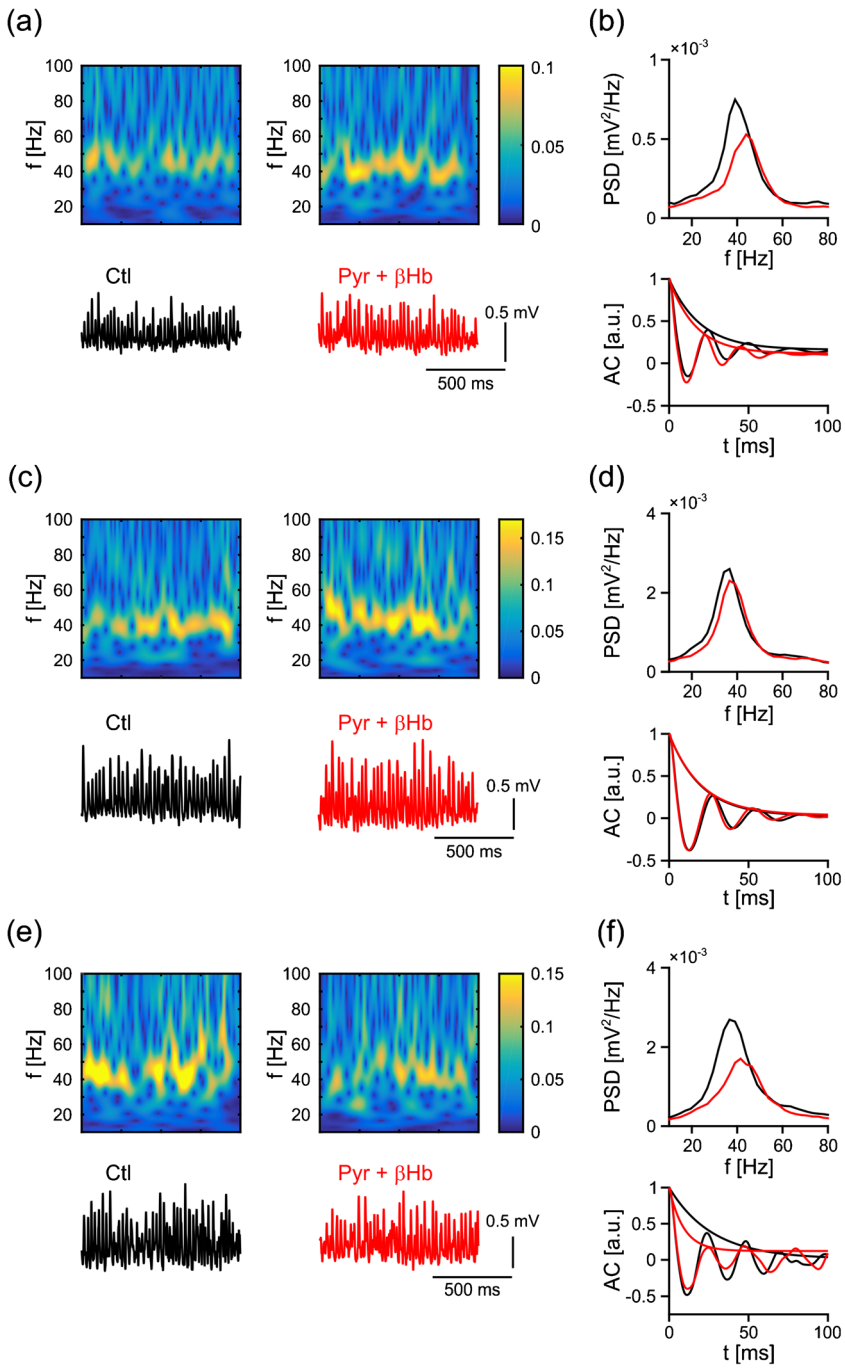

Fig. 2 Gamma oscillations fueled by different energy substrates. Gamma oscillations were recorded in ACSF with 10 mM glucose (Ctl, black) and, subsequently, in ACSF with 5 mM glucose, 5 mM pyruvate, and 4 mM β-hydroxybutyrate (Pyr + βHb, red). Recordings and analysis were made as shown in Fig. 1c–g. **a** Wavelet transform and corresponding sample traces of gamma oscillations in control (black trace) and Pyr + βHb (red trace) recorded in slice cultures at 11–14 DIV. **b** Power spectral density (PSD) and autocorrelation (AC) were computed from 3-min data segments of control (black curves) and Pyr + βHb (red curves). **c**, **d** Same as (**a**, **b**) for slice cultures at 28 DIV. **e**, **f** Same as (**a**, **b**) for slice cultures at 11–14 DIV, but under hyperoxic recording conditions (95% oxygen fraction)

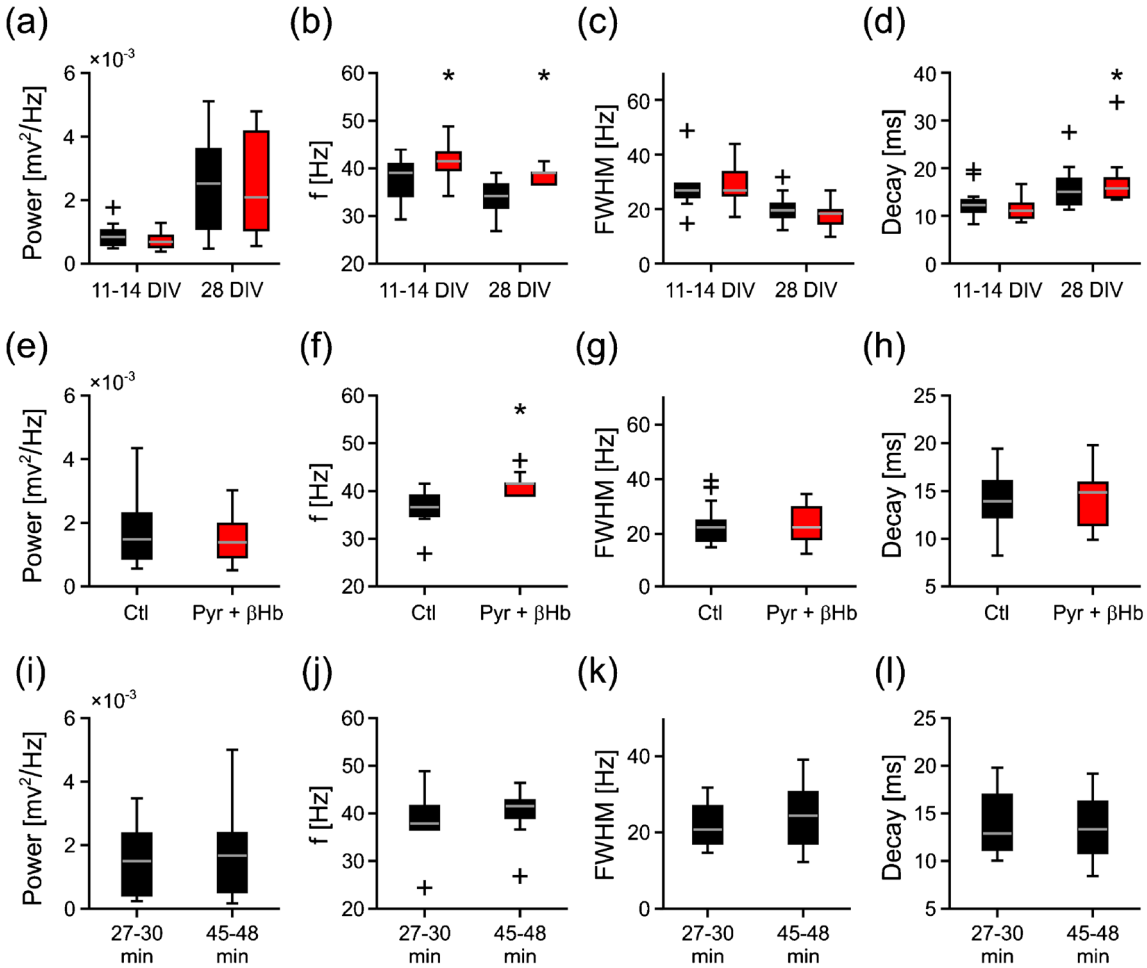

Fig. 3 Properties of gamma oscillations fueled by different energy substrates. Gamma oscillations as shown in Fig. 2 were analyzed for peak power (power), peak frequency (f), full width at half maximum (FWHM), and decay constant of the autocorrelation (decay). **a**–**d** The properties are shown for control (black boxplots) and Pyr + βHb (red boxplots) in slice cultures at 11–14 DIV ($n = 15$, $N = 3$) and 28 DIV ($n = 10$, $N = 3$) (Fig. 2a–d). **e**–**h** The properties are shown for control (Ctl, black boxplots) and Pyr + βHb (red boxplots) in slice cultures at 11–14 DIV under hyperoxic recording conditions (95% oxygen fraction) ($n = 23$, $N = 3$) (Fig. 2e, f). **i**–**l** The properties are shown for the time domains of 27 to 30 and 45 to 48 min (black boxplots) for slice cultures ($n = 12$, $N = 6$) that were continuously maintained in ACSF with 10 mM glucose (control condition). Paired *t* test and Wilcoxon signed rank test were used for statistical analysis. Statistical significance is marked by asterisks ($p < 0.05$)

control experiments made in the presence of 95% oxygen fraction (Fig. 2e, f, Fig. 3e–h). Such hyperoxic recording conditions have been commonly used to study neuronal activity on the cellular and network level [21, 26, 44], but they might affect energy metabolism, redox state, and synaptic activity [35, 42, 65].

These data show that partial substitution of glucose with pyruvate and the ketone body β-hydroxybutyrate increases the frequency of cholinergic gamma oscillations, independent of recording conditions and stage of tissue development.

Application of glutamine

We next explored the effects of the non-excitatory amino acid glutamine on gamma oscillations [4, 59]. Glutamine is the precursor of the excitatory neurotransmitter glutamate, and it is provided to neurons from astrocytes [34, 55]. After the induction of persistent gamma oscillations in ACSF without glutamine (deprivation of exogenous glutamine, "Materials and methods" section), we applied glutamine at a concentration of 1 mM [27, 30]. We note that during such exogenous deprivation, some glutamine and glycine (see below) might still be present at the synapse because of release from presynaptic nerve terminals and/or glial cells [6, 46].

Gamma oscillations persisted in the presence of glutamine. Power, frequency, FWHM, and decay of autocorrelation of gamma oscillations were unaffected (Fig. 4). Switches to other frequency bands or neural bursts were absent.

These data show that supplementation with the astrocytic precursor glutamine has no effect on the properties of cholinergic gamma oscillations.

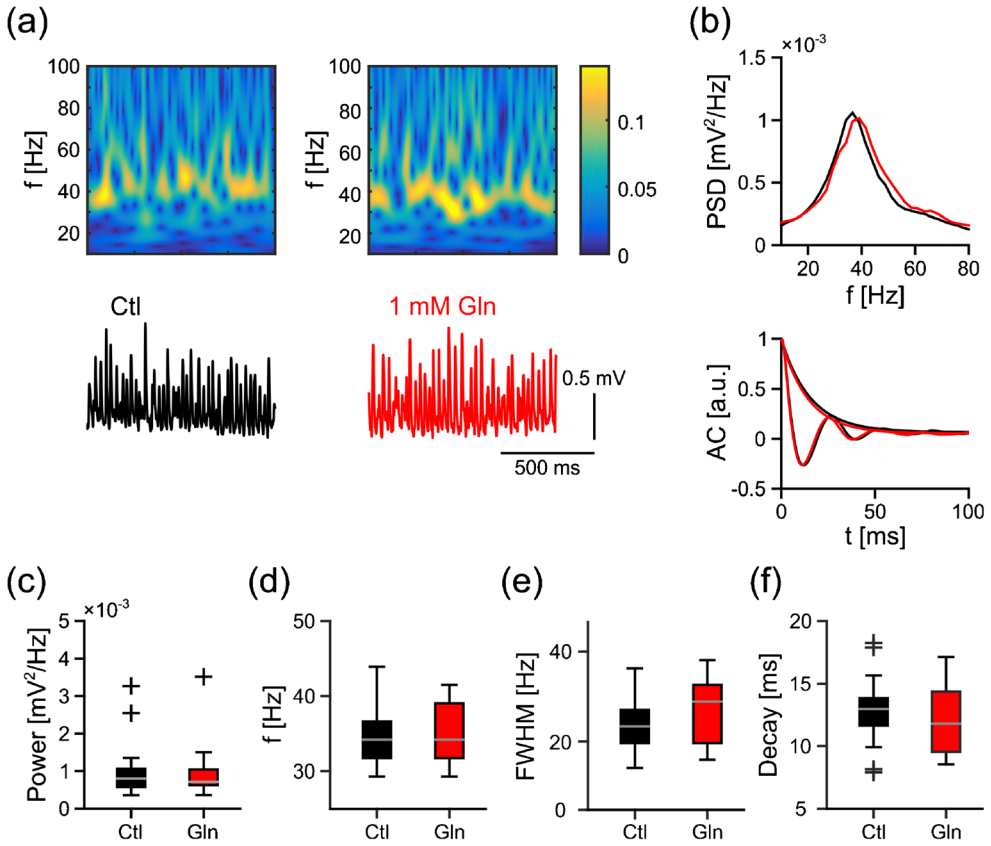

Fig. 4 Properties of gamma oscillations in the presence of glutamine. Gamma oscillations were recorded in ACSF (without exogenous glutamine) and, subsequently, in ACSF supplemented with glutamine. Recordings and analysis were made as shown in Fig. 1c–g. **a** Wavelet transform and corresponding sample traces of gamma oscillations in control (Ctl, black trace) and in the presence of 1 mM glutamine (red trace). **b** Power spectral density (PSD) and autocorrelation (AC) were computed from 3-min data segments of control (black curves) and glutamine (Gln, red curves). **c**–**f** Gamma oscillations were analyzed for peak power (power), peak frequency (f), full width at half maximum (FWHM), and decay constant of the autocorrelation (decay). The properties are shown for control (Ctl, black boxplots) and glutamine (Gln, red boxplots) in slice cultures ($n = 14$, $N = 2$). Paired t test and Wilcoxon signed rank test were applied for statistical analysis

Application of glycine

We next explored the effects of the amino acid glycine on gamma oscillations. In addition to its inhibitory action through ionotropic glycine receptors, glycine can modulate glutamatergic neurotransmission, e.g., in the hippocampus [39, 46, 50, 56]. Here, glycine serves as an essential co-agonist of glutamate and facilitates NMDA receptor-mediated currents. After the induction of persistent gamma oscillations in ACSF without glycine (deprivation of exogenous glycine, "Materials and methods" section), we applied exogenous glycine at non-toxic concentrations, i.e., 0.5 to 2.5 mM [7, 15, 58].

Gamma oscillations persisted in the presence of glycine (Fig. 5). Overall, power (Fig. 6a), frequency (Fig. 6b), and decay of autocorrelation (Fig. 6d) increased, whereas FWHM decreased (Fig. 6c). Notably, power and frequency of gamma oscillations did not change at the high concentration of glycine (2.5 mM). Switches to other frequency bands or neural bursts were absent [58].

In control experiments, we tested the modulation of gamma oscillations by glycine in the glutamatergic model of gamma oscillations, i.e., during continuous bath application of kainic acid (100 nM) [68]. We found that glycine (1.5 mM) decreased the frequency (26.9 ± 2.0 Hz in control versus 16.5 ± 3.1 Hz in the presence of glycine, $p < 0.01$), whereas subsequent application of strychnine (1 μM) had no significant effect (18.6 ± 3.0 Hz in the presence of glycine and strychnine, $p = 0.47$; $n = 8$, $N = 2$; one-way repeated-measures ANOVA with Holm-Sidak post-hoc test); other parameters were unchanged. Thus, the modulation of gamma oscillations differs in the glutamatergic and the cholinergic model, likely because the underlying synaptic mechanisms also differ significantly [45]. Moreover, the involvement of ligand-gated glycine receptors in the modulation of hippocampal gamma oscillations by glycine is unlikely.

These data show that supplementation with glycine increases power, frequency, and inner coherence of cholinergic gamma oscillations in a dose-dependent manner.

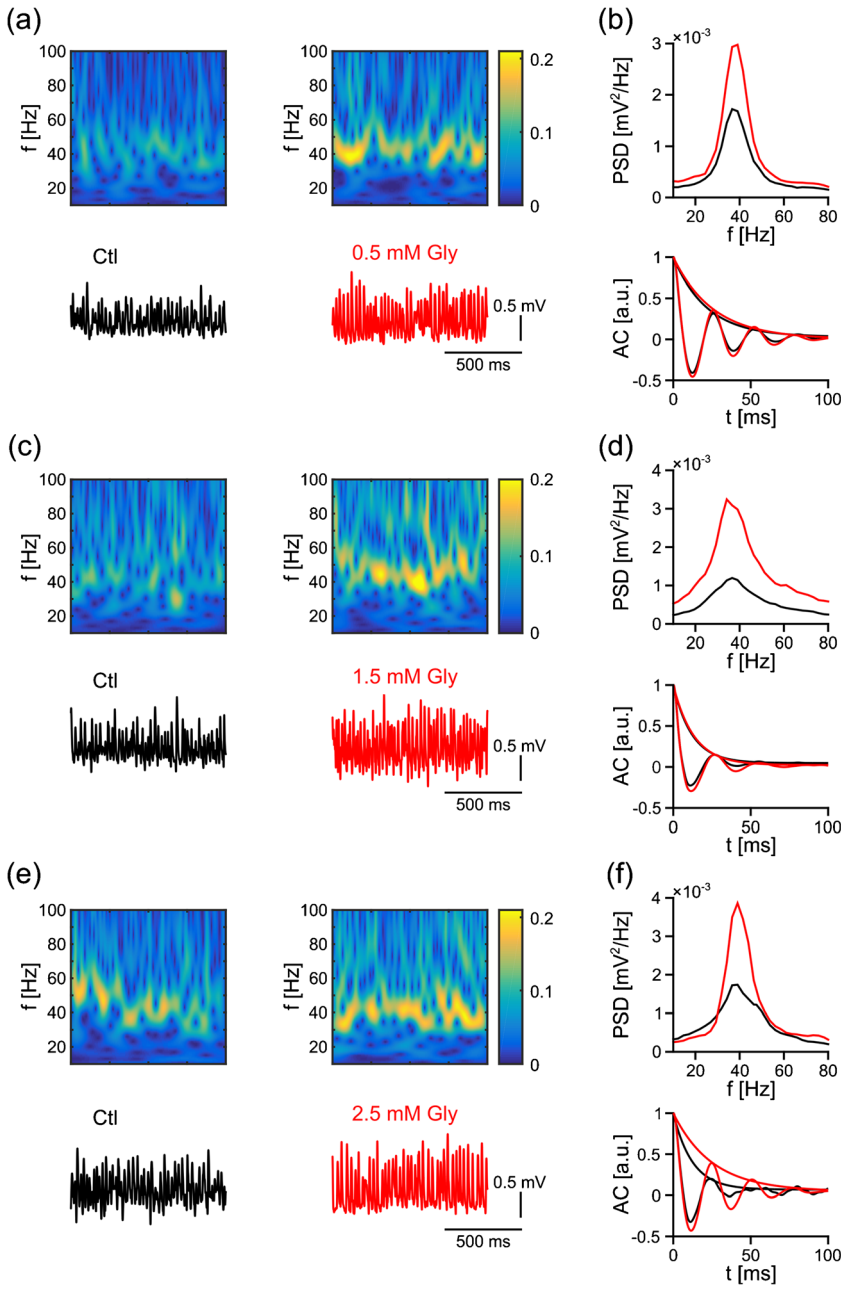

Fig. 5 Gamma oscillations in the presence of glycine. Gamma oscillations were recorded in ACSF (without exogenous glycine) and, subsequently, in ACSF supplemented with glycine. Recordings and analysis were made as shown in Fig. 1c–g. **a** Wavelet transform and corresponding sample traces of gamma oscillations in control (Ctl, black trace) and in the presence of glycine (Gly, red trace). **b** Power spectral density (PSD) and autocorrelation (AC) were computed from 3-min data segments of control (black curves) and 0.5 mM glycine (red curves). **c**, **d** Same as (**a**, **b**) for 1.5 mM glycine. **e**, **f** Same as (**a**, **b**) for 2.5 mM glycine

Discussion

Gamma oscillations in vivo and in vitro

Cortical gamma oscillations are functionally associated with neural information processing in vivo; they have a role in sensory perception, motor activity, memory formation, and attention [45, 76]. Gamma oscillations rely on precise synaptic transmission between excitatory principal cells and GABAergic interneurons, particularly parvalbumin-positive, fast-spiking basket cells [16, 23, 29]. In the hippocampus, inhibitory basket cells featuring extensive axon arbors contact the perisomatic region of pyramidal cells [29, 45, 74]. A recent study suggested that astrocytes may influence the properties of cortical gamma oscillations [48].

Persistent gamma oscillations have been reliably induced in acute hippocampal slices by bath application of cholinergic receptor agonists such as acetylcholine that mimics cholinergic neuronal input from the septum in vivo. Acetylcholine activates primarily muscarinic receptors in excitatory pyramidal cells and inhibitory GABAergic interneurons that interact through chemical and electrical synaptic mechanisms. Cholinergic receptor activation results in subthreshold membrane-potential fluctuations in neurons and concomitant network oscillations in local field potential recordings [29, 45, 74]. Gamma oscillations in hippocampal acute slices and slice

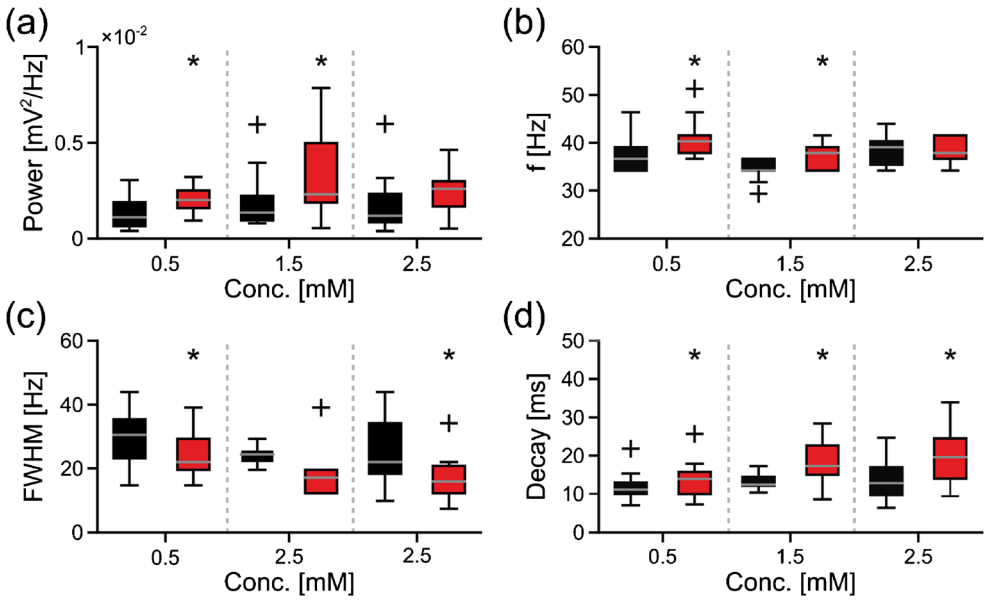

Fig. 6 Properties of gamma oscillations in the presence of glycine. Gamma oscillations as shown in Fig. 5 were analyzed for peak power (power), peak frequency (f), full width at half maximum (FWHM), and decay constant of the autocorrelation (decay). **a**–**d** The properties are shown for control (black boxplots) and for different concentrations of glycine (red boxplots) in slice cultures, i.e., 0.5 mM ($n = 16$, $N = 3$), 1.5 mM ($n = 12$, $N = 3$), or 2.5 mM ($n = 12$, $N = 3$). Paired t test and Wilcoxon signed Rank test were applied for statistical analysis. Statistical significance is marked by asterisks ($p < 0.05$)

cultures share many properties with hippocampal gamma oscillations in vivo, such as prominence in the intrinsic generator CA3 region, frequencies at around 40 Hz, and reversal of the field potential between *stratum pyramidale* and *stratum radiatum* [21, 41, 44, 64].

Effects of pyruvate and β-hydroxybutyrate on gamma oscillations

We show that partial substitution of glucose with pyruvate and the ketone body β-hydroxybutyrate increases the frequency of gamma oscillations, independent of recording conditions and stage of tissue development.

Hippocampal slices prepared from rat pups have been shown to maturate in vitro [12]. Notably, tissue development after slice preparation seems to be preprogrammed and largely independent of environmental factors, such as artificial culture medium and lack of any input from other brain areas [18]. Therefore, our data originate from slice cultures at two stages of maturation, roughly corresponding to the postnatal hippocampus 3 and 5 weeks after birth when the rat CA3 region is capable to express gamma oscillations [75]. In that, our experimental model might also cover some aspects of the physiological ketosis during the suckling period as well as physiological and pathophysiological situations after weaning in rats [57].

The physiological switch in energy metabolism after the suckling period is also reflected in the expression change of monocarboxylic acid transporters (MCTs). MCTs mediate fluxes of lactate, pyruvate, and ketone bodies across the blood-brain barrier as well as cell membranes of astrocytes, oligodendrocytes, and neurons [71, 77]. Ketone bodies, i.e., β-hydroxybutyrate, acetoacetate, and their breakdown product acetone, are synthesized in liver mitochondria from the oxidation of fatty acids derived from milk or adipose tissue during postnatal development, exhaustive physical exercise, long-term starvation, feeding a low-carbohydrate, high-fat ketogenic diet, or uncontrolled diabetes mellitus [1, 57, 67]. β-Hydroxybutyrate is formed reversibly from acetoacetate; it is a stable, water soluble, and nonvolatile compound that can be released into the blood. However, β-hydroxybutyrate can also be synthesized in astrocytes by oxidation of fatty acids or catabolism of amino acids [1, 20].

Previous reports from hippocampal slices showed that alternative energy substrates can sustain—or even enhance—energy metabolism and thus synaptic neuronal functions under certain experimental conditions [24, 37, 38, 70, 78]. However, in these studies, neuronal activation was induced by electrical stimulation paradigms of intrinsic hippocampal fiber pathways, associated with widely undefined neuronal network activity states. We report that physiologically occurring gamma oscillations show robustness against changes in the composition of available energy substrates on the qualitative level (gamma-band) as well as modulation on the quantitative level (frequency within the gamma-band). We made similar observations for the alternative energy substrate lactate [25]. This indicates that—in contrast to shortage in oxygen and nutrients [25, 30, 35, 41, 53]—gamma oscillations are relatively robust against changes in the composition of energy substrates, with relevance to postnatal development, physical exercise, starvation, certain diets, and diabetes mellitus.

Glutamine and gamma oscillations

Glutamate released at excitatory synapses must be rapidly removed from the extracellular space to permit fast and

precise neurotransmission and to prevent excitotoxicity. At glutamatergic synapses, most glutamate is taken up by adjacent astrocytes through excitatory amino acid transporters, EAAT1 (GLAST) and EAAT2 (GLT-1) [14, 49]. In astrocytes, glutamate is transformed into glutamine by the astrocyte-specific enzyme glutamine synthetase [6, 61]. Subsequently, glutamine is released into the extracellular space, taken up by neurons, and transformed back to glutamate by the enzyme phosphate-activated glutaminase (glutamate-glutamine cycle) [6, 52, 55]. In a similar fashion, the GABA-glutamine cycle has been proposed for the GABAergic synapse of inhibitory interneurons. However, supply with astrocytic glutamine might be functionally less important because inhibitory interneurons appear to feature larger reuptake of GABA [6, 34]. Indeed, cortical parvalbumin-positive basket cells, which are crucial for the generation of gamma oscillations in hippocampal and neocortical networks, express high levels of glutamic acid decarboxylase 65 (GAD65) and GAD67 for GABA synthesis as well as GABA membrane transporter 1 (GAT1) for GABA reuptake [22, 41].

We show that deprivation as well as supplementation with exogenous glutamine close to the physiological concentration range [27, 30] had no effect on the properties of gamma oscillations. This might indicate that the glutamate/GABA-glutamine cycle efficiently operates during gamma oscillations in slice cultures in our experimental model. In addition, the metabolism of glucose, lactate, and glycogen might support the synthesis of glutamine in astrocytes [34]. Our data are in line with observations made for paired-pulse evoked population responses in acute hippocampal slices; glutamine supplementation (0.5 mM) did not affect population spike amplitudes, whereas higher glutamine concentrations (2 to 5 mM) resulted in spreading depression [4]. Similarly, glutamine supplementation (0.9 and 4 mM) for up to 4 h did not change amplitude and frequency of miniature excitatory postsynaptic currents in acute hippocampal slices [40].

Effects of glycine on gamma oscillations

Glycine is a neurotransmitter involved in both inhibitory and excitatory neurotransmission in the CNS. Inhibitory glycinergic neurons have been found in many brain regions; however, they are most abundant in the brain stem and the spinal cord [9]. At excitatory synapses expressing NMDA receptors, glycine serves as an essential co-agonist of glutamate that increases the frequency of channel opening [39, 50, 56]. Glycine can be released into the synaptic cleft from glutamatergic axon terminals as well as from glial cells [31–33, 46]. In the hippocampus, glycine reuptake is mainly mediated through the electrogenic glycine transporter type 1 (GlyT1). GlyT1 is expressed in astrocytes but also co-localizes with NMDA receptors [5, 72, 79, 80]. Blockade of high-affinity GlyT1 modulates NMDA receptor-mediated responses and long-term potentiation by elevating extracellular glycine levels [51].

We show that deprivation of exogenous glycine did not affect the induction of persistent gamma oscillations, whereas subsequent glycine supplementation increased power, frequency, and inner coherence of cholinergic gamma oscillations in a dose-dependent manner. These findings might be explained by an increase in the amplitude of NMDA receptor-mediated currents in excitatory pyramidal cells and, perhaps, parvalbumin-positive GABAergic basket cells [41, 51, 58, 63]. The lack of these effects at the high concentration of glycine (2.5 mM) might reflect saturation of glycine uptake through GlyT1 and/or increased priming of NMDA receptors for internalization; the activation of inhibitory glycine receptors is less likely [10, 13, 15, 51, 60, 80].

Conclusion

We report that gamma oscillations show general robustness against changes in nutrient and amino acid composition of the extracellular fluid. However, the modulation of the properties of gamma oscillations may impact on cortical information processing under physiological and pathophysiological conditions.

Acknowledgements The authors thank Hasan Onur Dikmen for critical reading of the manuscript and helpful discussion.

Authors' contributions WV, JS, and OK designed the research; WV, JS, SE, JOH, and AL performed the research; WV, JS, SE, JOH, and AL analyzed the data; WV and OK wrote the manuscript. All authors have approved the final version of the manuscript and agree to be accountable for all aspects of the work.

Compliance with ethical standards

All applicable international, national, and/or institutional guidelines for the care and use of animals were followed.

Conflict of interest The authors declare that they have no conflict of interest.

References

1. Achanta LB, Rae CD (2017) β-Hydroxybutyrate in the brain: one molecule, multiple mechanisms. Neurochem Res 42:35–49. https://doi.org/10.1007/s11064-016-2099-2
2. Alberini CM, Cruz E, Descalzi G, Bessières B, Gao V (2017) Astrocyte glycogen and lactate: new insights into learning and memory mechanisms. Glia 66:1244–1262. https://doi.org/10.1002/glia.23250
3. Amaral AI (2013) Effects of hypoglycaemia on neuronal metabolism in the adult brain: role of alternative substrates to glucose. J Inherit Metab Dis 36:621–634. https://doi.org/10.1007/s10545-012-9553-3

4. An JH, Su Y, Radman T, Bikson M (2008) Effects of glucose and glutamine concentration in the formulation of the artificial cerebrospinal fluid (ACSF). Brain Res 1218:77–86. https://doi.org/10.1016/j.brainres.2008.04.007
5. Aroeira RI, Sebastião AM, Valente CA (2014) GlyT1 and GlyT2 in brain astrocytes: expression, distribution and function. Brain Struct Funct 219:817–830. https://doi.org/10.1007/s00429-013-0537-3
6. Bak LK, Schousboe A, Waagepetersen HS (2006) The glutamate/GABA-glutamine cycle: aspects of transport, neurotransmitter homeostasis and ammonia transfer. J Neurochem 98:641–653
7. Barth A, Nguyen LB, Barth L, Newell DW (2005) Glycine-induced neurotoxicity in organotypic hippocampal slice cultures. Exp Brain Res 161:351–357
8. Bélanger M, Allaman I, Magistretti PJ (2011) Brain energy metabolism: focus on astrocyte-neuron metabolic cooperation. Cell Metab 14:724–738. https://doi.org/10.1016/j.cmet.2011.08.016
9. Betz H, Gomeza J, Armsen W, Scholze P, Eulenburg V (2006) Glycine transporters: essential regulators of synaptic transmission. Biochem Soc Trans 34:55–58
10. Brackmann M, Zhao C, Schmieden V, Braunewell KH (2004) Cellular and subcellular localization of the inhibitory glycine receptor in hippocampal neurons. Biochem Biophys Res Commun 324:1137–1142
11. Buzsáki G, Buhl DL, Harris KD, Csicsvari J, Czéh B, Morozov A (2003) Hippocampal network patterns of activity in the mouse. Neuroscience 116:201–211
12. Caeser M, Aertsen A (1991) Morphological organization of rat hippocampal slice cultures. J Comp Neurol 307:87–106
13. Chattipakorn SC, McMahon LL (2002) Pharmacological characterization of glycine-gated chloride currents recorded in rat hippocampal slices. J Neurophysiol 87:1515–1525
14. Chaudhry FA, Lehre KP, van Lookeren Campagne M, Ottersen OP, Danbolt NC, Storm-Mathisen J (1995) Glutamate transporters in glial plasma membranes: highly differentiated localizations revealed by quantitative ultrastructural immunocytochemistry. Neuron 15:711–720
15. Chen RQ, Wang SH, Yao W, Wang JJ, Ji F, Yan JZ, Ren SQ, Chen Z, Liu SY, Lu W (2011) Role of glycine receptors in glycine-induced LTD in hippocampal CA1 pyramidal neurons. Neuropsychopharmacology 36:1948–1958. https://doi.org/10.1038/npp.2011.86
16. Cunningham MO, Whittington MA, Bibbig A, Roopun A, LeBeau FE, Vogt A, Monyer H, Buhl EH, Traub RD (2004) A role for fast rhythmic bursting neurons in cortical gamma oscillations in vitro. Proc Natl Acad Sci U S A 101:7152–7157
17. Dalsgaard MK, Secher NH (2007) The brain at work: a cerebral metabolic manifestation of central fatigue? J Neurosci Res 85:3334–3339
18. De Simoni A, Griesinger CB, Edwards FA (2003) Development of rat CA1 neurones in acute versus organotypic slices: role of experience in synaptic morphology and activity. J Physiol 550:135–147
19. Dienel GA (2012) Brain lactate metabolism: the discoveries and the controversies. J Cereb Blood Flow Metab 32:1107–1138. https://doi.org/10.1038/jcbfm.2011.175
20. Edmond J, Robbins RA, Bergstrom JD, Cole RA, de Vellis J (1987) Capacity for substrate utilization in oxidative metabolism by neurons, astrocytes, and oligodendrocytes from developing brain in primary culture. J Neurosci Res 18:551–561
21. Fisahn A, Pike FG, Buhl EH, Paulsen O (1998) Cholinergic induction of network oscillations at 40 Hz in the hippocampus in vitro. Nature 394:186–189
22. Fish KN, Sweet RA, Lewis DA (2011) Differential distribution of proteins regulating GABA synthesis and reuptake in axon boutons of subpopulations of cortical interneurons. Cereb Cortex 21:2450–2460. https://doi.org/10.1093/cercor/bhr007
23. Galarreta M, Hestrin S (2002) Electrical and chemical synapses among parvalbumin fast-spiking GABAergic interneurons in adult mouse neocortex. Proc Natl Acad Sci U S A 99:12438–12443
24. Galeffi F, Foster KA, Sadgrove MP, Beaver CJ, Turner DA (2007) Lactate uptake contributes to the NAD(P)H biphasic response and tissue oxygen response during synaptic stimulation in area CA1 of rat hippocampal slices. J Neurochem 103:2449–2461
25. Galow LV, Schneider J, Lewen A, Ta TT, Papageorgiou IE, Kann O (2014) Energy substrates that fuel fast neuronal network oscillations. Front Neurosci 8:398. https://doi.org/10.3389/fnins.2014.00398
26. Geiger JR, Bischofberger J, Vida I, Fröbe U, Pfitzinger S, Weber HJ, Haverkampf K, Jonas P (2002) Patch-clamp recording in brain slices with improved slicer technology. Pflugers Arch 443:491–501
27. Gjessing LR, Gjesdahl P, Sjaastad O (1972) The free amino acids in human cerebrospinal fluid. J Neurochem 19:1807–1808
28. Gonzalez SV, Nguyen NH, Rise F, Hassel B (2005) Brain metabolism of exogenous pyruvate. J Neurochem 95:284–293
29. Gulyás AI, Szabó GG, Ulbert I, Holderith N, Monyer H, Erdélyi F, Szabó G, Freund TF, Hájos N (2010) Parvalbumin-containing fast-spiking basket cells generate the field potential oscillations induced by cholinergic receptor activation in the hippocampus. J Neurosci 30:15134–15145. https://doi.org/10.1523/JNEUROSCI.4104-10.2010
30. Hájos N, Mody I (2009) Establishing a physiological environment for visualized in vitro brain slice recordings by increasing oxygen supply and modifying aCSF content. J Neurosci Methods 183:107–113. https://doi.org/10.1016/j.jneumeth.2009.06.005
31. Harsing LG Jr, Matyus P (2013) Mechanisms of glycine release, which build up synaptic and extrasynaptic glycine levels: the role of synaptic and non-synaptic glycine transporters. Brain Res Bull 93:110–119. https://doi.org/10.1016/j.brainresbull.2012.12.002
32. Hayashi Y, Ishibashi H, Hashimoto K, Nakanishi H (2006) Potentiation of the NMDA receptor-mediated responses through the activation of the glycine site by microglia secreting soluble factors. Glia 53:660–668
33. Henneberger C, Papouin T, Oliet SH, Rusakov DA (2010) Long-term potentiation depends on release of D-serine from astrocytes. Nature 463:232–236. https://doi.org/10.1038/nature08673
34. Hertz L, Rothman DL (2016) Glucose, lactate, β-hydroxybutyrate, acetate, GABA, and succinate as substrates for synthesis of glutamate and GABA in the glutamine-glutamate/GABA cycle. Adv Neurobiol 13:9–42
35. Huchzermeyer C, Albus K, Gabriel HJ, Otáhal J, Taubenberger N, Heinemann U, Kovács R, Kann O (2008) Gamma oscillations and spontaneous network activity in the hippocampus are highly sensitive to decreases in pO2 and concomitant changes in mitochondrial redox state. J Neurosci 28:1153–1162. https://doi.org/10.1523/JNEUROSCI.4105-07.2008
36. Huchzermeyer C, Berndt N, Holzhütter HG, Kann O (2013) Oxygen consumption rates during three different neuronal activity states in the hippocampal CA3 network. J Cereb Blood Flow Metab 33:263–271. https://doi.org/10.1038/jcbfm.2012.165
37. Ivanov A, Zilberter Y (2011) Critical state of energy metabolism in brain slices: the principal role of oxygen delivery and energy substrates in shaping neuronal activity. Front Neuroenerg 3:9. https://doi.org/10.3389/fnene.2011.00009
38. Izumi Y, Ishii K, Katsuki H, Benz AM, Zorumski CF (1998) Beta-hydroxybutyrate fuels synaptic function during development. Histological and physiological evidence in rat hippocampal slices. J Clin Invest 101:1121–1132
39. Johnson JW, Ascher P (1987) Glycine potentiates the NMDA response in cultured mouse brain neurons. Nature 325:529–531
40. Kam K, Nicoll R (2007) Excitatory synaptic transmission persists independently of the glutamate-glutamine cycle. J Neurosci 27:9192–9200

41. Kann O (2016) The interneuron energy hypothesis: implications for brain disease. Neurobiol Dis 90:75–85. https://doi.org/10.1016/j.nbd.2015.08.005
42. Kann O, Kovács R (2007) Mitochondria and neuronal activity. Am J Physiol Cell Physiol 292:C641–C657
43. Kann O, Schuchmann S, Buchheim K, Heinemann U (2003) Coupling of neuronal activity and mitochondrial metabolism as revealed by NAD(P)H fluorescence signals in organotypic hippocampal slice cultures of the rat. Neuroscience 119:87–100
44. Kann O, Huchzermeyer C, Kovács R, Wirtz S, Schuelke M (2011) Gamma oscillations in the hippocampus require high complex I gene expression and strong functional performance of mitochondria. Brain 134:345–358. https://doi.org/10.1093/brain/awq333
45. Kann O, Papageorgiou IE, Draguhn A (2014) Highly energized inhibitory interneurons are a central element for information processing in cortical networks. J Cereb Blood Flow Metab 34:1270–1282. https://doi.org/10.1038/jcbfm.2014.104
46. Kirischuk S, Héja L, Kardos J, Billups B (2016) Astrocyte sodium signaling and the regulation of neurotransmission. Glia 64:1655–1666. https://doi.org/10.1002/glia.22943
47. Künnecke B, Cerdan S, Seelig J (1993) Cerebral metabolism of [1,2-13C2]glucose and [U-13C4]3-hydroxybutyrate in rat brain as detected by 13C NMR spectroscopy. NMR Biomed 6:264–277
48. Lee HS, Ghetti A, Pinto-Duarte A, Wang X, Dziewczapolski G, Galimi F, Huitron-Resendiz S, Piña-Crespo JC, Roberts AJ, Verma IM, Sejnowski TJ, Heinemann SF (2014) Astrocytes contribute to gamma oscillations and recognition memory. Proc Natl Acad Sci U S A 111:E3343–E3352. https://doi.org/10.1073/pnas.1410893111
49. Lehre KP, Danbolt NC (1998) The number of glutamate transporter subtype molecules at glutamatergic synapses: chemical and stereological quantification in young adult rat brain. J Neurosci 18:8751–8757
50. Li Y, Krupa B, Kang JS, Bolshakov VY, Liu G (2009) Glycine site of NMDA receptor serves as a spatiotemporal detector of synaptic activity patterns. J Neurophysiol 102:578–589. https://doi.org/10.1152/jn.91342.2008
51. Martina M, Gorfinkel Y, Halman S, Lowe JA, Periyalwar P, Schmidt CJ, Bergeron R (2004) Glycine transporter type 1 blockade changes NMDA receptor-mediated responses and LTP in hippocampal CA1 pyramidal cells by altering extracellular glycine levels. J Physiol 557:489–500
52. Marx MC, Billups D, Billups B (2015) Maintaining the presynaptic glutamate supply for excitatory neurotransmission. J Neurosci Res 93:1031–1044. https://doi.org/10.1002/jnr.23561
53. McIlwain H (1951) Metabolic response in vitro to electrical stimulation of sections of mammalian brain. Biochem J 49:382–393
54. McKenna MC (2012) Substrate competition studies demonstrate oxidative metabolism of glucose, glutamate, glutamine, lactate and 3-hydroxybutyrate in cortical astrocytes from rat brain. Neurochem Res 37:2613–2626. https://doi.org/10.1007/s11064-012-0901-3
55. McKenna MC, Stridh MH, McNair LF, Sonnewald U, Waagepetersen HS, Schousboe A (2016) Glutamate oxidation in astrocytes: roles of glutamate dehydrogenase and aminotransferases. J Neurosci Res 94:1561–1571. https://doi.org/10.1002/jnr.23908
56. Minota S, Miyazaki T, Wang MY, Read HL, Dun NJ (1989) Glycine potentiates NMDA responses in rat hippocampal CA1 neurons. Neurosci Lett 100:237–242
57. Nehlig A (2004) Brain uptake and metabolism of ketone bodies in animal models. Prostaglandins Leukot Essent Fatty Acids 70:265–275
58. Newell DW, Barth A, Ricciardi TN, Malouf AT (1997) Glycine causes increased excitability and neurotoxicity by activation of NMDA receptors in the hippocampus. Exp Neurol 145:235–244
59. Nishimura F, Nishihara M, Mori M, Torii K, Takahashi M (1995) Excitability of neurons in the ventromedial nucleus in rat hypothalamic slices: modulation by amino acids at cerebrospinal fluid levels. Brain Res 691:217–222
60. Nong Y, Huang YQ, Ju W, Kalia LV, Ahmadian G, Wang YT, Salter MW (2003) Glycine binding primes NMDA receptor internalization. Nature 422:302–307
61. Papageorgiou IE, Gabriel S, Fetani AF, Kann O, Heinemann U (2011) Redistribution of astrocytic glutamine synthetase in the hippocampus of chronic epileptic rats. Glia 59:1706–1718. https://doi.org/10.1002/glia.21217
62. Papageorgiou IE, Lewen A, Galow LV, Cesetti T, Scheffel J, Regen T, Hanisch UK, Kann O (2016) TLR4-activated microglia require IFN-γ to induce severe neuronal dysfunction and death in situ. Proc Natl Acad Sci U S A 113:212–217. https://doi.org/10.1073/pnas.1513853113
63. Papp OI, Karlócai MR, Tóth IE, Freund TF, Hájos N (2013) Different input and output properties characterize parvalbumin-positive basket and axo-axonic cells in the hippocampal CA3 subfield. Hippocampus 23:903–918. https://doi.org/10.1002/hipo.22147
64. Penttonen M, Kamondi A, Acsády L, Buzsáki G (1998) Gamma frequency oscillation in the hippocampus of the rat: intracellular analysis in vivo. Eur J Neurosci 10:718–728
65. Pomper JK, Graulich J, Kovacs R, Hoffmann U, Gabriel S, Heinemann U (2001) High oxygen tension leads to acute cell death in organotypic hippocampal slice cultures. Brain Res Dev Brain Res 126:109–116
66. Roberts EL Jr (2007) The support of energy metabolism in the central nervous system with substrates other than glucose. In: Lajtha A, Gibson GE, Dienel GA (eds) Handbook of neurochemistry and molecular neurobiology. Brain energetics. Integration of molecular and cellular processes, 3rd edn. Springer, Berlin, pp 137–179
67. Rojas-Morales P, Tapia E, Pedraza-Chaverri J (2016) β-Hydroxybutyrate: a signaling metabolite in starvation response? Cell Signal 28:917–923. https://doi.org/10.1016/j.cellsig.2016.04.005
68. Schneider J, Lewen A, Ta TT, Galow LV, Isola R, Papageorgiou IE, Kann O (2015) A reliable model for gamma oscillations in hippocampal tissue. J Neurosci Res 93:1067–1078. https://doi.org/10.1002/jnr.23590
69. Schneider J, Berndt N, Papageorgiou IE, Maurer J, Bulik S, Both M, Draguhn A, Holzhütter HG, Kann O (2017) Local oxygen homeostasis during various neuronal network activity states in the mouse hippocampus. J Cereb Blood Flow Metab. https://doi.org/10.1177/0271678X17740091
70. Schurr A, West CA, Rigor BM (1988) Lactate-supported synaptic function in the rat hippocampal slice preparation. Science 240:1326–1328
71. Simpson IA, Carruthers A, Vannucci SJ (2007) Supply and demand in cerebral energy metabolism: the role of nutrient transporters. J Cereb Blood Flow Metab 27:1766–1791
72. Smith KE, Borden LA, Hartig PR, Branchek T, Weinshank RL (1992) Cloning and expression of a glycine transporter reveal colocalization with NMDA receptors. Neuron 8:927–935
73. Stenkamp K, Palva JM, Uusisaari M, Schuchmann S, Schmitz D, Heinemann U, Kaila K (2001) Enhanced temporal stability of cholinergic hippocampal gamma oscillations following respiratory alkalosis in vitro. J Neurophysiol 85:2063–2069
74. Traub RD, Bibbig A, Fisahn A, LeBeau FE, Whittington MA, Buhl EH (2000) A model of gamma-frequency network oscillations induced in the rat CA3 region by carbachol in vitro. Eur J Neurosci 12:4093–4106

75. Tsintsadze V, Minlebaev M, Suchkov D, Cunningham MO, Khazipov R (2015) Ontogeny of kainate-induced gamma oscillations in the rat CA3 hippocampus in vitro. Front Cell Neurosci 9: 195. https://doi.org/10.3389/fncel.2015.00195
76. Uhlhaas PJ, Singer W (2010) Abnormal neural oscillations and synchrony in schizophrenia. Nat Rev Neurosci 11:100–113. https://doi.org/10.1038/nrn2774
77. Vannucci SJ, Simpson IA (2003) Developmental switch in brain nutrient transporter expression in the rat. Am J Physiol Endocrinol Metab 285:E1127–E1134
78. Yamane K, Yokono K, Okada Y (2000) Anaerobic glycolysis is crucial for the maintenance of neural activity in guinea pig hippocampal slices. J Neurosci Methods 103:163–171
79. Zafra F, Aragón C, Olivares L, Danbolt NC, Giménez C, Storm-Mathisen J (1995) Glycine transporters are differentially expressed among CNS cells. J Neurosci 15:3952–3969
80. Zhang LH, Gong N, Fei D, Xu L, Xu TL (2008) Glycine uptake regulates hippocampal network activity via glycine receptor-mediated tonic inhibition. Neuropsychopharmacology 33:701–711